Arsenic trioxide and lead acetate induce apoptosis in adult rat hepatic stem cells

Soumik Agarwal · Sonali Roy · Atish Ray ·
Shibnath Mazumder · Shelley Bhattacharya

Abstract In the present study, the toxicity of arsenic trioxide and lead acetate was assessed in adult hepatic stem cells induced in the 2-acetyl-aminofluorene/partial hepatectomy rat model. Isolated oval cells were incubated separately for 6 h with 40 µM each of arsenic trioxide and lead acetate. 3-(4,5-Dimethylthiazole-2-yl)-2,5-diphenyltetrazolium bromide assay denoted significant time-dependent cell death in arsenic and lead treated oval cells. The degree of stress imposed by these metals was evidenced by induction of heat shock protein (HSP) 70 and HSP 90. Arsenic and lead were found to trigger apoptosis as revealed by DNA ladder formation, Western blots of apoptotic factors, and reverse transcriptase polymerase chain reaction analyses of bax and bcl-2. Results clearly indicate that both arsenic and lead induced apoptosis is caspase-mediated and accompanied by extracellular signal-regulated kinase (ERK) dephosphorylation. Full-length BH3-interacting-domain death agonist expression in presence of caspase 3 inhibitor unravels a direct involvement of caspase in As and Pb induced apoptosis. Expression patterns of apoptosis inducing factor, B cell lymphoma-2 (Bcl-2) antagonist of cell death, Bcl-2-associated X protein, and Bcl2 also signify mitochondrial regulation of apoptosis effected by lead and arsenic. It is concluded that stimulation of caspase cascade and simultaneous ERK dephosphorylation are the most significant operative pathways directly associated with apoptotic signals triggered by arsenic and lead in the oval cells.

Keywords Apoptosis · Arsenic · Lead · Liver · Oval cell

S. Agarwal · A. Ray · S. Bhattacharya (✉)
Environmental Toxicology Laboratory,
Department of Zoology, Visva-Bharati University,
Santiniketan 731235, India
e-mail: bhattacharyashelley@rediffmail.com

S. Mazumder
Immunobiology Laboratory,
Department of Zoology, Visva-Bharati University,
Santiniketan 731235, India

Present address:
S. Roy
Ocean Research Institute, University of Tokyo,
Tokyo, Japan

Abbreviations

AAF	2-acetylaminofluorene
AIF	Apoptosis-inducing factor
AP-1	Activator protein-1
Apaf-1	Apoptotic protease activating factor-1
Bcl-2	B cell lymphoma-2
Bax	Bcl-2-associated X protein
Bad	Bcl-2 antagonist of cell death
Bid	BH3-interacting-domain death agonist
CK-19	cytokeratin 19
DMA	Dimethylarsinic acid

DMEM   Dulbecco's minimum essential medium
ERK   Extracellular signal-regulated kinase
GAPDH   Glyceraldehyde phosphate dehydrogenase
HBSS   Hanks balanced salt solution
HSP   Heat shock protein
MMA   Monomethylarsonic acid
MTT   3-(4,5-dimethylthiazole-2-yl)-2,
         5-diphenyltetrazolium bromide
NFkB   Nuclear factor kB
OV1   Oval cell marker 1
OV6   Oval cell marker 6
PH   Partial hepatectomy
RT PCR   Reverse transcriptase polymerase chain
         reaction
SCF   Stem cell factor
ZFL   Zebra fish liver cell line

Introduction

Stem cells are defined by their ability of self-renewal and differentiation potential and classified into two major categories, pluripotent embryonic stem cells and adult stem cells, which are also known as mesenchymal stem cells or multipotent adult progenitor cells (Lanza 2006). Adult liver is known to regenerate by hepatocytes reentering into cell cycle after surgical resection or injury (Fausto 2001; Best and Coleman 2007). Liver transplant model has demonstrated that hepatocytes are functional stem cells of liver having the potential of clonal expansion (Alison et al. 2001). It has been proposed that adult liver contains facultative hepatic stem cells or progenitor cells located in the Canal of Hering, which, if induced, proliferate as a subpopulation called oval cell to restore the liver mass (Qin et al. 2004). Oval cells have aroused considerable interest because of their therapeutic potential in liver, tissue engineering, and gene therapy in liver-related diseases (He et al. 2004). They are characterized by the presence of specific markers in rat, such as cytokeratin (CK) 8, 14, 18, and 19 (Marceau 1990) and oval cell marker (OV)-1 and OV-6 (Dunsford and Sell 1989). Liver being the main detoxifying organ is prone to injury by exposure to xenobiotics. The level of stress imposed by xenobiotics may be assessed by the profile of heat shock protein (HSP) 70 and HSP 90 which are highly conserved proteins playing important roles in stressed and unstressed cells (Parsell and Lindquist 1993; Nollen and Morimoto 2002). Various toxicants lead to different anomalies, such as cell death, teratogenesis, carcinogenesis, as well as premature aging and the diseases of aging (Trosko 2003), which is dependent on the homeostatic regulation of cell proliferation, differentiation, apoptosis, and senescence of hepatocytes. Therefore, the profile of these proteins has been studied to assess the level of stress imposed by the metals.

Arsenic, a metalloid universally distributed in nature, is considered to be one of the most toxic xenobiotics. There are several reports demonstrating toxic effects of arsenic in liver. Exposure of humans, experimental animals, and cultured cells to arsenic results in a variety of diverse health effects, dysfunction of critical enzymes, and cell damage. Paradoxically among xenobiotics, arsenic can both cause and cure cancer (Kann et al. 2005; Look 1998; Liu and Huang 2005). A common molecular mechanism related to length (chronic vs. acute), level (high dose vs. low dose), and/or species of arsenic (arsenite, arsenate, monomethylarsonic acid, dimethylarsinic acid) exposure may exist in the anticarcinogenic and carcinogenic actions of arsenic (Ayala-Fierro et al. 1999). It has been reported that exposure to more than 200 μM arsenite or arsenate resulted in apoptosis by 44.5–61.5% of the JB6Cl41 cell types, respectively (Chen et al. 2000). Ten micromolars and 20 μM of arsenic trioxide were found to induce apoptosis and 40 μM of arsenic increased the rate of cell death (Milton et al. 2004).

Lead is one of the most ubiquitous elements and after initial absorption is distributed in blood, liver, kidney, and bone. Following prolonged exposure, lead burden is found mainly in the hematopoietic and nervous systems. However, lead exposure has been shown to induce apoptosis in hepatocytes (Columbano et al. 1985) and like arsenic, there are reports indicating the role of lead in inducing both anticytotoxic and antimutagenic effects through persistent activation of extracellular signal-regulated kinase (ERK)1/2 (Lin et al. 2003).

Various xenobiotics can cause apoptosis in different cell types through primary activation of caspase-dependent or caspase-independent pathways (Pulido and Parrish 2003). Loss of mitochondrial transmembrane potential is the initial event leading to apoptosis (Petit et al. 1996). Instability of the mitochondrial membrane results in release of cytochrome c which binds to apoptotic protease-activating factor 1, the

adaptor protein of caspase 9 to form the apoptosome. This event amplifies the caspase signaling by activating caspase 3. The mitogen-activated protein kinases (MAPKs), extracellular signal-regulated kinase, JUN N-terminal kinase (JNK), and p38 also take part in this event leading to activation of activator protein-1 or the nuclear factor kappa B. Arsenic and lead induced apoptosis has been reported by various authors using hepatocytes but, to the best of our knowledge, has not been studied in freshly isolated rat hepatic stem cells or oval cells. On the other hand, the unlimited proliferation ability, the plasticity to generate other cell types and its therapeutic potential (Davila et al. 2004) encouraged us to assess the effects of sublethal exposure to arsenic and lead in the oval cells induced in the acetoaminofluoride/partial hepatectomy (AAF/PH) rat model. In the present investigation, an attempt was made to elucidate the cellular responses to subcritical concentrations of arsenic and lead in the oval cells.

Materials and methods

Chemicals

The primary antibody, antiheat shock protein 70 and 90 (raised in mouse), ammonium persulfate, Coomassie brilliant blue, phenylmethylsulfonyl fluoride (PMSF), Nonidet, N-(-2-fluorenyl) acetamide, collagenase type-IV, deoxyribonuclease I, hyaluronidase, insulin, dexamethasone, and Apoptosis polymerase chain reaction (PCR) B cell lymphoma-2 (Bcl-2)-associated X protein (Bax)/Bcl-2 Multiplex Primer Sets were procured from Sigma Chemical Co. (St. Louis, MO, USA). Other primary antibodies to full length caspase 3, full length caspase 9, apoptosis-inducing factor (AIF), Bax, BH3-interacting-domain death agonist (Bid), Bcl-2 antagonist of cell death (Bad), Bcl2 (raised in rabbit), ERK, JNK, and p38 (raised in mouse) CK-19 and stem cell factor (SCF; raised in goat) were purchased from Santa Cruz Biotechnology Inc. (Santa Cruz, CA, USA). The molecular weight marker kit for polyacrylamide gel electrophoresis was purchased from Fermentas Life Sciences (Hanover, MD, USA). Rabbit anti-mouse IgG linked to alkaline phosphatase was procured from Bangalore Genei Pvt. Ltd. (Bangalore, India).The SV Total RNA Isolation System and caspase inhibitor

(Ac-DEVD-cho) was procured from Promega Corporation (Madison, WI, USA). First strand cDNA Synthesis kit was procured from Fermentas Life Sciences. Actinase-E was procured from Kaken Pharmaceuticals Company (Tokyo, Japan). All other chemicals used were, of analytical grade, purchased from Sisco Research Laboratories (Mumbai, India) and E. Merck (Mumbai, India).

Animals and their maintenance

Male white rats (*Rattus norvegicus*) of the Sprague Dawley strain having a body weight of 125 to 150 g were procured from a single animal supplier to minimize differences in the population of rats supplied. Rats were acclimatized for at least 7 days prior to the investigation and housed in a temperature controlled animal room (Inglis 1980), where they were fed with rat chow and water ad libitum. All experiments were approved by the Animal Care Committee of Visva-Bharati University and performed in accordance with the criterion outlined.

Induction and isolation of oval cell

Oval cells were induced in the AAF/PH rat model (Shimano et al. 2003). Briefly, AAF was administered daily to rats by gavage at 15 mg.kg^{-1} body weight for 4 days. On day 5, a standard two third PH was carried out, and then the daily administration of AAF at the same dosage continued for 5 days. All surgical procedures were done under anesthesia by using anesthetic ether. Oval cells were isolated by a two-step collagenase digestion method (Shimano et al. 2003). The purity of the oval cells was determined by the presence of oval cell specific marker (CK-19) and also a stem cell marker (SCF) and found to be 95% pure (data not shown).

Experimental design

We observed that both As and Pb at 40 μM concentration resulted in 20% death of the isolated oval cells, respectively, at 6 h of treatment. Therefore, in the present investigation, this exposure concentration was selected to assess the apoptotic mechanism manifested by arsenic and lead.

Oval cells (3×10^6 ml^{-1}) were added in 2 ml of Dulbecco's minimum essential medium (GIBCO) in

24-well culture plates and treated with 40 μM of arsenic or lead at 37°C in a CO_2 incubator set at 5%. The incubations were terminated at 1, 2, 4, and 6 h, the cells washed with Hanks balanced salt solution, and a thin smear prepared on glass slides for routine eosin–hematoxylin observation. Unexposed cells served as the concurrent control.

Assessment of cytotoxicity

Xenobiotic induced cell death was determined at selected time intervals postincubation by trypan blue (0.4%) dye exclusion test (Brambilla and Martelli 1995) demonstrating 95–98% survival of the unexposed cells. Cytotoxicity of arsenic and lead exposure for 6 h at the concentration of 40 μM was determined by the standard MTT assay. Results were calculated as percentage cell death against control and expressed as mean±SE of three individual MTT assays (Supino 1995). Statistical analysis was done following two-way analysis of variance (Snedecor and Cochran 1967).

Isolation and analysis of DNA

The genomic DNA of rat oval cell was isolated using the solvent (phenol, chloroform, isoamyl alcohol) extraction method (Sambrook et al. 1989) and run on 1.2% agarose gel using bromophenol blue as the tracking dye and visualized in a Bio Rad Gel Doc System.

Reverse transcription and polymerase chain reaction analysis

Total cellular RNA from rat oval cells was isolated using the SV Total RNA Isolation System (Promega Corporation) as per the manufacturer's guideline. The PCR primers used were 5′-CAT CTT CTT CCA GAT GGT GA-3′ (3′ antisense); 5′-GTT TCA TCC AGG ATC GAG CAG-3′ (5′sense) for *bax*; 5′-GAG ACA GCC AGG AGA AAT CA-3′ (3′ antisense); 5′-CCT GTG GAT GAC TGA GTA CC-3′ (5′sense) for *bcl-2*; glyceraldehyde phosphate dehydrogenase primers served as internal control in the assay. Control reactions without template were also included with amplification for each pair of primer and the reverse transcriptase (RT)-PCR analysis was performed following the manufacturer's guideline (Sigma Chemical Co.) in an Eppendorf Master Cycler.

Preparation of sample for Western blots

Oval cells (3×10^6 cells ml^{-1}) were sonicated in 50 mM Tris buffer (pH 7.6) containing 0.1 mM PMSF and 1% Nonidet and centrifuged at 10,000 ×*g* for 20 min. The cytosolic supernatant was carefully collected, passed through 0.2 μm filters, the protein content determined (Lowry et al. 1951), and stored at −80°C until further use. Fifty micrograms protein from control and exposed oval cells were subjected to 10% sodium dodecyl sulfate polyacrylamide gel electrophoresis analysis at a constant voltage (Laemmli 1970) and transferred to polyvinylidene fluoride membranes (Roy and Bhattacharya 2006). The blots were incubated with the antibodies mentioned above and developed using alkaline phosphatase conjugated rabbit anti-mouse and goat anti-rabbit secondary antibodies.

Caspase inhibition studies

In the present studies, caspase activity was inhibited by the inhibitor Ac-DEVD-cho at 2 h of metal treatment considering the maximum response elicited by the oval cells at this time point. Oval cells were cotreated with arsenic trioxide (40 μM) and the caspase inhibitor (10 μM) in one set and with lead acetate (40 μM) and caspase inhibitor (10 μM) in another for 2 h and expression patterns of *bax* and *bcl-2* were investigated in caspase 3 inhibitor treated samples to detect the involvement of various factors in As and Pb induced apoptosis

Results

Detection of oval cells

Isolated oval (Fig. 1a) cells generated by AAF/PH were confirmed to be oval cells by the double positive response towards the well-known markers of CK 19 and SCF (Fig. 1b,c).

Cytotoxicity of As and Pb

The oval cells demonstrated 80% survival as compared to the unexposed cells after 6 h of metal treatment. Metal treatments recorded highest rate of cell death between 1 and 2 h of arsenic and between 4
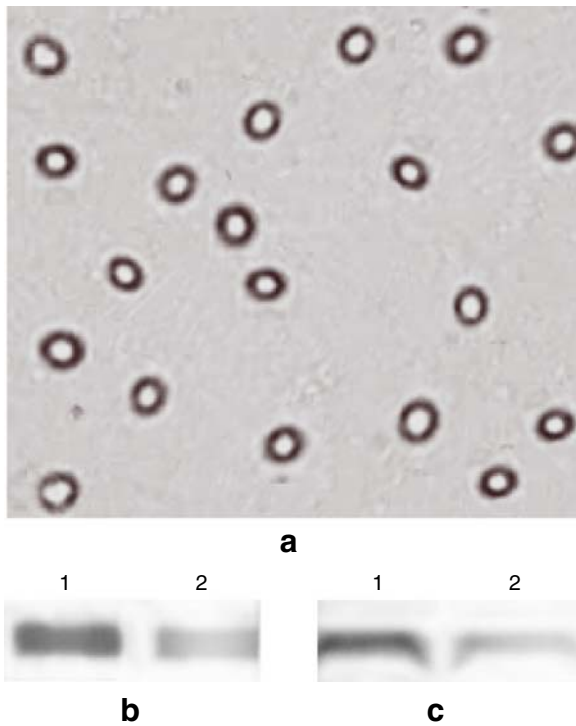
Fig. 1 a Oval cells (original magnification, ×100). b Western blot of CK 19. c Western blot of SCF. *Lane 1*—oval cell; *lane 2*—differentiated hepatocyte from different population

and 6 h of lead treatment (Fig. 2a). Apoptotic changes noted in the treated cells were significant (Fig. 2c,d) as compared to the unexposed oval cells (Fig. 2b).

Apoptotic DNA fragmentation

Significant intranucleosomal pattern was denoted by As treatment at 1 h. However, low molecular weight DNA fragments were not observed in 6 h arsenic exposed cell which could be due to rapid degradation corroborating our microscopic observation of arsenic-exposed oval cells (figure not shown). In Pb treated cells, however, DNA degradation took place more gradually and an intranucleosomal DNA fragmentation was apparent only at 6 h (Fig. 3a,b).

Induction of stress proteins and caspase dependent pathway

In As treated oval cells, there was no change in the expression of HSP 70 until 1 h of incubation, thereafter, its expression heightened while HSP 90 level moderately increased until 4 h followed by a decline at 6 h of treatment. Contrastingly, Pb treated cells demonstrated a remarkable induction of HSP 70 at 1 h followed by a sharp decrease until the end of the experiment. In Pb treatment, HSP 90 was maximally induced within 1 h and, thereafter, it declined reaching a value below that of the control at 6 h (Fig. 4a,b).

In As treatment, the expression of procaspase 3 was found to be high throughout the incubation which was more noteworthy at 1 h. On the other hand, there was a lower level of expression of procaspase 3 in Pb treated cells after 1 h of treatment (Fig. 4a,b). As seen with procaspase 3, the level of procaspase 9 also increased with time in As treated cells and the rate of increase was remarkable at 2 h of incubation. In Pb treatment, the response manifested was depletion of procaspase 9 until 2 h of incubation reaching the control level at 6 h.

Fig. 2 a MTT assay of As (40 μM) and Pb (40 μM) treated oval cells pooled from six rats for each replicate (mean±SE). *$p<0.05$ indicates significant difference from the control. b Untreated oval cell. c Arsenic treated oval cell showing apoptotic nuclear fragmentation. d Lead treated oval cell showing apoptotic nuclear fragmentation
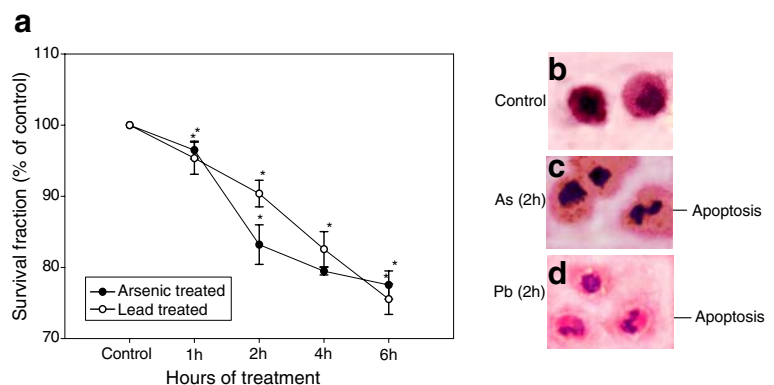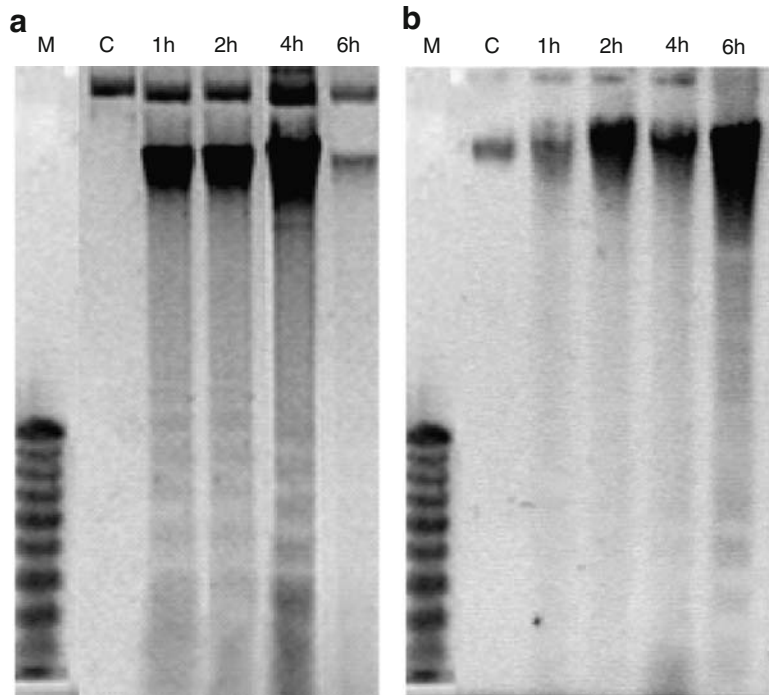
Fig. 3 DNA ladder formation of control and treated oval cell. **a** Arsenic treated (40 μM); **b** lead treated (40 μM)

The overall pERK expression level remained low throughout the experimental durations in As and Pb treatments. In the case of pp38, the expression demonstrated an increase until 2 h followed by a decline, even below that of the control, at 4 and 6 h of As treatment. In contrast, Pb treated oval cells demonstrated a biphasic pattern where the expression level of pp38 was higher than that of the control at 1, 2, and 6 h of incubation (Fig. 4a,b).
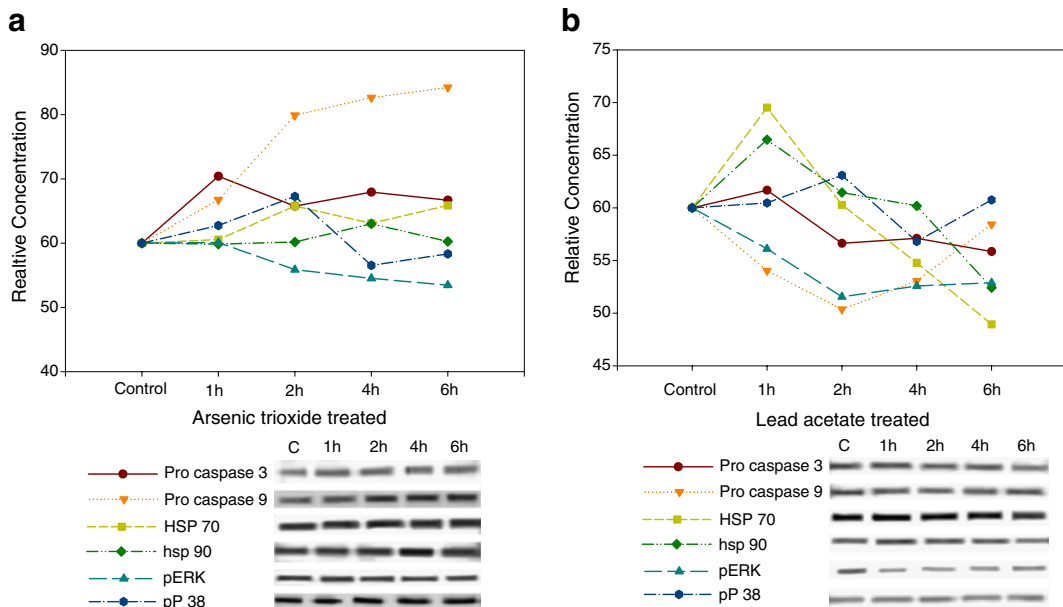

Fig. 4 a WB and densitometric analysis of As treated cells. **b** WB and densitometric analysis of Pb treated cells

Expression of mitochondrial factors

In arsenic treatment, AIF level declined at 1 h followed by an increasing trend which reached the basal level at 6 h. Bid level showed a slight increase until 2 h, regaining the control level at 4 and 6 h. Other factors, such as Bad, had a similar trend of expression demonstrating a decrease at 1 h followed by an increase at 4 h and again a reduced expression at 6 h (Fig. 5a,b).Contrastingly, in lead treated cells, AIF level was found to be low throughout the experimental duration. Expression level of Bad was remarkably high until 2 h of incubation declining below that of the control at 6 h while Bid expression followed a typical biphasic pattern (Fig. 5a,b).

RT-PCR analysis of *bax* and *bcl-2*

To further clarify the scheme of events in both the metal treatments, we have investigated the changes in *bax* and *bcl-2* transcription levels by RT-PCR. It was demonstrated that the induced expression of *bcl-2* occurred transiently at 1 h only which continued to decrease till the end of the experiment (Fig. 6a,b).

Caspase inhibitor treated cells also demonstrated an overexpressed *bcl-2* level. Overexpression of *bax* in the oval cell was significant at 1 h of lead treatment which is noteworthy at 4 and 6 h of As treatment (Fig. 6a,b). In the presence of the caspase inhibitor, *bax* expression in both As and Pb treated oval cells was found to be suppressed.

Inhibition of pro- and antiapoptotic factors

In presence of caspase inhibitor, procaspase 3 concentrations in Pb treated cells did not record any significant change from the control although a slight increase was noted in case of As treated cells. Procaspase 9 was remarkably suppressed in As treated cells in the presence of caspase inhibitor at 2 h as against the incubation without caspase inhibitor. On the other hand, in Pb treated oval cells, suppression of procaspase 9 was not evident (Fig. 7a,b).

In As treated cells, caspase inhibitor did not demonstrate any remarkable change in AIF expression but its induction was evident in Pb treated cells. Again, in the presence of caspase inhibitor, increase in Bid level was manifested in As treated cells but not in the Pb treated ones. In respect of Bad, there was a remarkable increase in As treated oval cells while in Pb treated oval cells, Bad was significantly suppressed (Fig. 7a,b). Interestingly, caspase inhibitor reduced both Bax and Bcl-2 expression in arsenic and lead treated cells but in Pb treatment, the presence of caspase inhibitor caused the Bcl-2 level to fall even below the untreated control (data not shown).

Discussion

Heat shock proteins (Hsp 70 and Hsp 90) have been widely accepted as stress responsive proteins. They
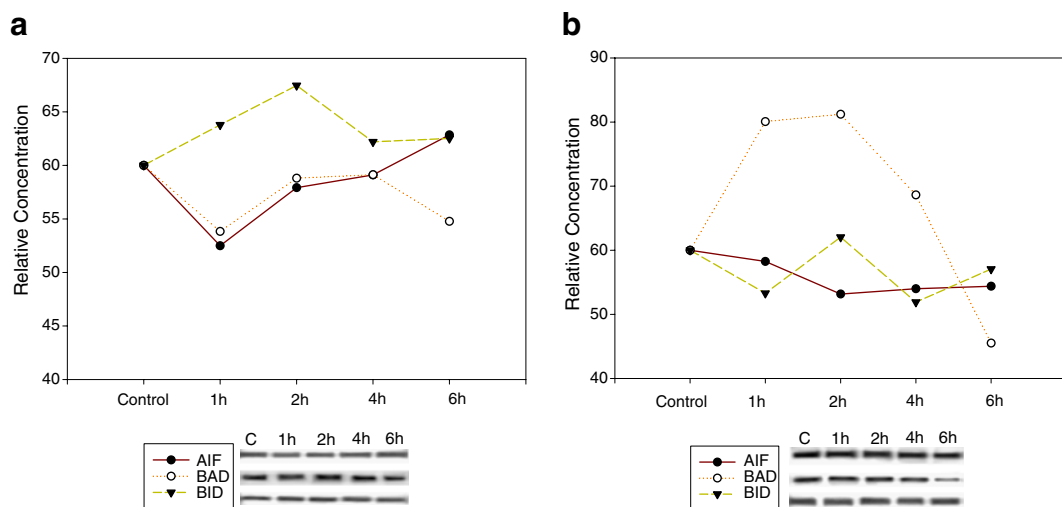

Fig. 5 **a** WB and densitometric analysis of As treated cells. **b** WB and densitometric analysis of Pb treated cells
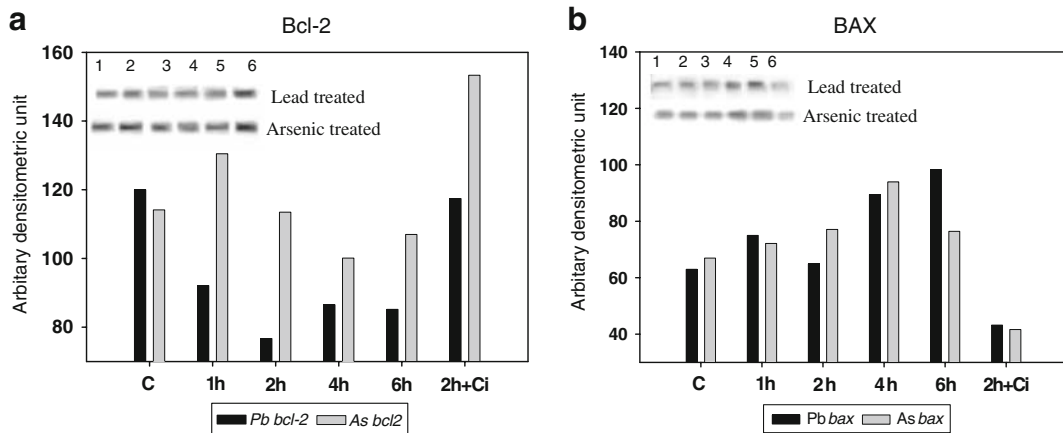
Fig. 6 RT-PCR analysis: expression profile of **a** Bcl-2 and **b** Bax; *Lane 1*, control; *lane 2*, 1 h; *lane 3*, 2 h; *lane 4*, 4 h; *lane 5*, 6 h; *lane 6*, 10 μM caspase inhibitor cotreated

represent a family of proteins comprised of constitutive and inducible members (Lindquist and Craig 1998) which have been reported to confer protection to cells from prior heat shock or other agents of stress (Subjeck et al. 1982; Li and Werb 1982). The antiapoptotic role of Hsp 70 has already been clarified in hepatocytes (Ikeyama et al. 2001). Recently, it was reported that 30 μM arsenite induced massive apoptosis in Zebra fish line cells where Hsp 70 was found to be a sensitive biomarker (Seok et al. 2007). We observed that As induced Hsp 70 gradually while Pb had a more immediate effect suggesting the ability of the oval cells to survive in the stress imposed by the candidate metals. On the other hand, Hsp 90 appears to be more constitutively expressed in the oval cells.

It is known that apoptosis involves both caspase activation and mitochondrial alteration leading to release of caspase activators (Wang 2002; Adams 2003; Green and Kroemer 2004). In the present study, the DNA ladder of nucleosomal pattern, the widely accepted hallmark of caspase-3 mediated apoptosis, clearly indicates that apoptosis has initiated within an hour of arsenic exposure corroborating our recent in vivo study in arsenic exposed fish (Datta et al. 2007). The same phenomenon is also evident in the Pb treated oval cells although after a protracted incubation.

The caspase profile revealed that the level of procaspase 3, one of the most important executioner caspases, overexpressed at 1 h of As exposure after which the rate of activation and the rate of production
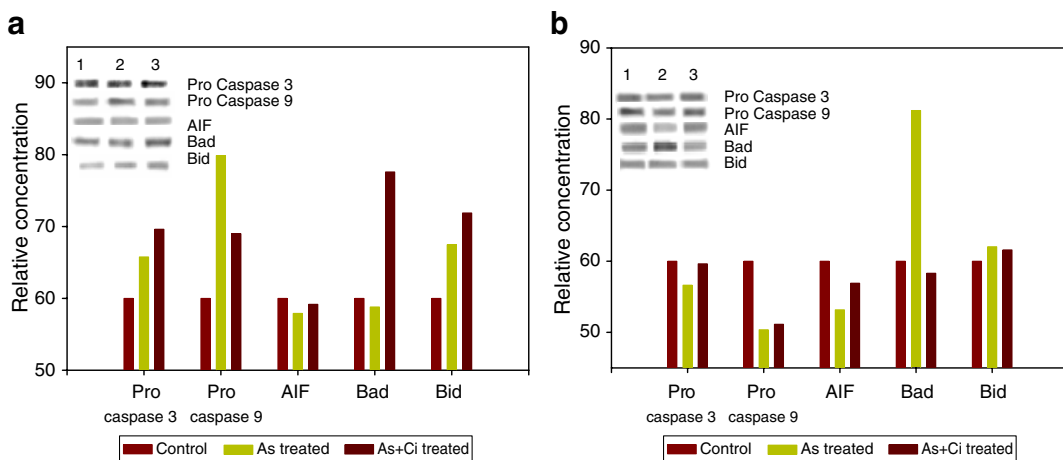

Fig. 7 a WB and densitometric analysis of As treated cells. **b** WB and densitometric analysis of Pb treated cells

remained static. On the other hand, procaspase 3 in Pb treated cells was also overexpressed initially but its breakdown occurred during the later phase of the incubation which clearly indicates the enhancement of the apoptotic pathway by Pb.

In both As and Pb treated cells, high rate of procaspase 9 synthesis took place suggesting a role of caspase 9 pathway in induction of apoptosis in oval cells on exposure to these xenobiotics. Interestingly, inhibition of procaspase 3 reduces synthesis of procaspase 9 and enhances the procaspase 3 level setting up a self amplification loop as proposed earlier in Jurkat T cells, clone E6-1 (Sun et al. 1999). Thus, it may be surmised that As and Pb induced apoptosis in rat oval cell is mediated by caspase 9 supporting the contention that caspase 3 activation is dependent on critical concentration of caspase 9 (Earnshaw et al. 1999).

Mitogen-activated protein kinases, the family of serine threonine kinases, are important signaling mediators of cellular stress response via regulation of different genes related to apoptosis. In earlier studies, it has been shown that p38 MAP kinase is a well-known member in stress-activated signal transduction (Waskiewicz and Cooper 1995; Robinson and Cobb 1997) and ERK activation is strongly enhanced by overexpression of p38 (Ludwig et al. 1998). There are reports that ERK and p38 play a vital role in arsenic induced apoptosis in a time dependent manner (Bode and Dong 2002) and JNK 2 was found to be critical for activation of the mitochondrial death pathway, Bid cleavage, and mitochondrial translocation (Liedtke and Trautwein 2006). In the present study, the increase in pp38 levels at the earlier stages of metal exposure suggests its initial contribution to withstand both As and Pb induced stress in the oval cells. The decrease in pp38 and pERK levels with increase in the duration of As exposure clearly indicates the predominating effect of apoptosis over survival. Thus, dephosphorylation of p38 and ERK seems to be most significant for triggering apoptosis in both As treated oval cells as reported earlier in other cell types (Kapur et al. 2002; Lin et al. 2003; Boudreau et al. 2007).

Mitochondrial transmembrane potential plays a key role in cell death where selective release of mediators amplify apoptosis and profound loss of mitochondrial function leads to necrosis (Petit et al. 1996) and mitochondria incorporating Bax were found to release

AIF selectively. After being activated by apoptotic stimuli, AIF is released from mitochondria and cause DNA breakage (Li et al. 2001; Bidère et al. 2003). In the present study, initial reduction in AIF level in the cytosolic fraction confirms the role of this factor in DNA breakage; although in the later stage of incubation, arsenic induces AIF synthesis at a much higher rate and does not significantly change the AIF status as compared to that of lead. Moreover, findings from caspase inhibition study demonstrate that contribution of AIF is more vital in Pb induced apoptosis.

In earlier studies, it has been reported that mitochondrial membrane permeability is regulated through *bcl 2* family of protooncogenes, antiapoptotic (*bcl-2*), and proapoptotic (*bad*, *bax*) (Tsujimoto and Shimizu 2001). Normally, Bax remains in the cytosol, but on being activated by apoptotic stimuli, it translocates and is inserted in mitochondria thereby increasing its permeability. In the present study, stimulation of Bax synthesis is evident during the later phase of incubation with As, which event has been amply elucidated by RT-PCR. In Pb treated oval cells, also RT-PCR analysis clearly demonstrates stimulation of Bax expression at the earlier phase of incubation, while Bcl2 suppression is apparent throughout the incubation. We have also judged the patterns of RT-PCR of Bax and Bcl 2, in the presence of caspase inhibitor. Bax suppression is noteworthy in both Pb and As treated cells. Caspase inhibitor results in significant overexpression of *bcl 2* indicating the direct contribution of caspase 3 over mitochondrial regulation.

The BH3 domain-only protein Bid, a death agonist member of the Bcl-2/Bcl-xl family (Wang et al. 1996), is localized in the cytosolic fraction as an inactive precursor (Li et al. 1998; Luo et al. 1998) and upon proteolytic cleavage truncated Bid also translocates to mitochondria to release cytochrome C (Gross et al. 1999; Yin et al. 1999). Our study reveals that As induces Bid synthesis at the initial phase while in the case of Pb treatment, the expression appears to be biphasic. Again, in the presence of caspase inhibitor, substantial increase in the cytosolic Bad concentration occurs in As treated oval cells only. This clearly indicates cytosolic sequestration of Bad in As treated oval cell. Contrastingly, in case of Pb treatment, the negtive regulatory role of caspase 3 inhibition on Bad is evident. On the other hand, there is no siginificant involvement of Bid in Pb induced apoptosis of oval

cell but caspase 3 inhibition demonstrates a direct role of of Bid activation only in As treated cells.

From our study, it is evident that in contrast to Hsp 90, Hsp 70 plays a major role in the recovery of metal-induced stress in the adult hepatic stem cells. Earlier studies of Mosser et al. (1997, 2000) have shown that Hsp70 acts as a chaperone for protection against stress-induced apoptosis by interfering with downstream activity of procaspase 9 and 3. Roy and Bhattacharya (2006) had also observed concomitant inhibition of hepatocyte apoptosis coupled with enhanced Hsp70 expression following in vivo exposure of fish to As_2O_3. It is further concluded that in the metal treated oval cells, the caspase cascade is the most significant operative pathway amplifying the mitochondrial apoptotic signals and phosphorylation of the survival factor, p38, essentially allows the cells to recover. Besides activation of the caspase cascade, increasing rate of dephosphorylation of the survival factor Erk is also found to have an essential role in induction of apoptosis in arsenic and lead treated oval cells.

References

Adams JM. Ways of dying: multiple pathways to apoptosis. Genes Dev. 2003;17:2481–95.

Alison MR, Poulsom R, Forbes SJ. Update on hepatic stem cells. Liver 2001;21:367–73.

Ayala-Fierro F, Barber DS, Rael LT, Carter DE. In vitro tissue specificity for arsine and arsenite toxicity in the rat. Toxicol Sci. 1999;52:122–29.

Best DH, Coleman WB. Treatment with 2-AAF blocks the small hepatocyte-like progenitor cell response in retrorsine-exposed rats. J Hepatol. 2007;46:1055–63.

Bidère N, Lorenzo HK, Carmona S, Laforge M, Harper F, Dumont C, et al. Cathepsin D triggers Bax activation, resulting in selective apoptosis-inducing factor (AIF) relocation in T lymphocytes entering the early commitment phase to apoptosis. J Biol Chem. 2003;278:31401–11.

Bode AM, Dong Z. The paradox of arsenic: molecular mechanisms of cell transformation and chemotherapeutic effects. Crit Rev Oncol Hematol. 2002;42:5–24.

Boudreau RTM, Conrad DM, Hoskin DW. Apoptosis induced by protein phosphatase 2A (PP2A) inhibition in T leukemia cell is negatively regulated by PP2A—associated p38 mitogen-activated protein kinase. Cell Signal. 2007;19:139–51.

Brambilla G, Martelli A. Cytotoxicity, DNA fragmentation and DNA repair synthesis in primary human hepatocytes. In: O'Hare S, Atterwill CK, editors. In vitro toxicity testing protocols. Totowa, New Jersey: Humana; 1995. p. 59–66.

Chen N-Y, Ma W-Y, Yang CS, Dong Z. Inhibition of arsenite-induced apoptosis and AP-1 activity by epigallocatechin-3-gallate and theoflavins. J Environ Pathol Toxicol Oncol. 2000;19:287–95.

Columbano A, Ledda-Columbano GM, Coni PP, Faa G, Liguori C, Santa Cruz G, et al. Occurrence of cell death (apoptosis) during the involution of liver hyperplasia. Lab Invest. 1985;52:670–5.

Datta S, Saha DR, Ghosh D, Majumdar T, Bhattacharya S, Mazumder S. Sub-lethal concentration of arsenic interferes with the proliferation of hepatocytes and induces in vivo apoptosis in Clarias batrachus L. Comp Biochem Physiol Part C. 2007;145:339–49.

Davila JC, Cezar GG, Thiede M, Strom S, Miki T, Trosko J. Use and application of stem cells in toxicology. Toxicol Sci. 2004;79:214–23.

Dunsford HC, Sell S. Production of monoclonal antibodies to preneoplastic liver cell populations induced by chemical carcinogen in rats and transplantable Morris hepatomas. Cancer Res. 1989;49:4887–93.

Earnshaw WC, Martins LM, Kaufmann SH. Mammalian caspases: structure, activation, substrates, and functions during apoptosis. Annu Rev Biochem. 1999;68:383–424.

Fausto N. Liver regeneration: from laboratory to clinic. Liver Transplant. 2001;276:835–44.

Green DR, Kroemer G. The pathophysiology of mitochondrial cell death. Science 2004;305:626–9.

Gross A, Yin XM, Wang K, Wei MC, Jockel J, Milliman C, et al. Caspase cleaved BID targets mitochondria and is required for cytochrome c release, while BCL-XL prevents this release but not tumor necrosis factor-R1/Fas death. J Biol Chem. 1999;274:1156–63.

He ZP, Tan WQ, Tang YF, Zhang HJ, Feng MF. Activation, isolation, identification and in vitro proliferation of oval cells from adult rat livers. Cell Prolif. 2004;37:177–87.

Ikeyama S, Kusumoto K, Miyake H, Rokutan K, Tashiro S. A non-toxic heat shock protein 70 inducer, geranylgeranylacetone, suppresses apoptosis of cultured rat hepatocytes caused by hydrogen peroxide and ethanol. J Hepatol. 2001;55:53–61.

Inglis JK. Introduction to laboratory animal science and technology. 1st ed. Oxford: Pergamon; 1980. p. 37–126.

Kann S, Estes C, Reichard JF, Huang M, Sartor MA, Schwemberger S, et al. Butylhydroquinone protects cells genetically deficient in glutathione biosynthesis from arsenite-induced apoptosis without significantly changing their prooxidant status. Toxicol Sci. 2005;87:365–84.

Kapur R, Chandra S, Cooper R, McCarthy J, Williams DA. Role of p38 and ERK MAP kinase in proliferation of erythroid progenitors in response to stimulation by soluble and membrane isoforms of stem cell factor. Blood 2002;100:1287–93.

Laemmli UK. Cleavage of structural proteins during the assembly of the head of bacteriophage T4. Nature 1970;227:680–5.

Lanza R. Essentials of stem cell biology. USA: Elsevier; 2006.

Li GC, Werb Z. Correlation between the synthesis of heat shock proteins and the development of thermotolerance in Chinese hamster fibroblasts. Proc Natl Acad Sci USA. 1982;79:3218–22.

Li H, Zhu H, Xu CJ, Yuan J. Cleavage of BID by caspase 8 mediates the mitochondrial damage in the Fas pathway of apoptosis. Cell 1998;94:491–501.

Li L, Luo X, Wang X. Endonuclease G is an apoptotic DNase when released from mitochondria. Nature 2001;412:95–9.

Liedtke C, Trautwein C. The role of JNK2 in toxic liver injury. J Hepatol. 2006;45:762–4.

Lin YW, Chuang SM, Yang JL. Persistent activation of ERK1/2 by lead acetate increases nucleotide excision repair synthesis and confers anti-cytotoxicity and anti-mutagenicity. Carcinogenesis 2003;24:53–61.

Lindquist S, Craig EA. The heat shock proteins. Annu Rev Genet. 1998;22:631–37.

Liu ZM, Huang HS. As_2O_3-induced c-Src/EGFR/ERK signaling is via Sp1 binding sites to stimulate p21WAF1/CIP1 expression in human epidermoid carcinoma A431 cells. Cell Signal. 2005;18:244–55.

Look AT. Arsenic and apoptosis in the treatment of acute promyelocytic leukemia. J Natl Cancer Inst. 1998;90:86–8.

Lowry OH, Rosebrough NJ, Farr AL, Randall RJ. Measurement of protein with the Folin phenol reagent. J Biol Chem. 1951;193:265–75.

Ludwig S, Hoffmeyer A, Goebeler M, Kilian K, Hafner H, Neufeld B, et al. The stress inducer arsenite activates mitogen-activated protein kinases extracellular signal-regulated kinases 1 and 2 via a MAPK kinase 6/p38-dependent pathway. J Biol Chem. 1998;273:1917–22.

Luo X, Budiharjo H, Zou H, Slaughter C, Wang X. Bid, a Bcl2 interacting protein, mediates cytochrome c release from mitochondria in response to activation of cell surface death receptors. Cell 1998;94:481–90.

Marceau N. Biology of disease. Cell lineage and differentiation programs in epidermal; urothelial and hepatic tissues and their neoplasms. Lab Invest. 1990;63:4–20.

Milton AG, Zalewski PD, Ratnaike RN. Zinc protects against arsenic-induced apoptosis in a neuronal cell line, measured by DEVD-caspase activity. Biometals 2004;17:707–13.

Mosser DD, Caron AW, Bourget L, Larose CD, Massie B. Role of the human heat shock protein hsp70 in protection against stress-induced apoptosis. Mol Cell Bio. 1997;17:5317–27.

Mosser DD, Caron AW, Bourget L, Meriin AB, Sherman AY, Morimoto RI, et al. The chaperone function of hsp70 is required for protection against stress-induced apoptosis. Mol Cell Biol. 2000;20:7146–59.

Nollen EA, Morimoto RI. Chaperoning signaling pathways: molecular chaperones as stress-sensing 'heat shock' proteins. J Cell Sci. 2002;115:2809–16.

Parsell DA, Lindquist S. The function of heat-shock proteins in stress tolerance: degradation and reactivation of damaged proteins. Annu Rev Genet. 1993;27:437–96.

Petit PX, Susin SA, Zamzami N, Mignotte B, Kroemer G. Mitochondria and programmed cell death: back to the future. FEBS Lett. 1996;396:7–13.

Pulido MD, Parrish AR. Metal-induced apoptosis: mechanisms. Mutat Res. 2003;533:227–41.

Qin AL, Zhou XQ, Zhang W, Yu H, Xie Q. Characterization and enrichment of hepatic progenitor cells in adult rat liver. World J Gastroenterol. 2004;10:1480–6.

Robinson MJ, Cobb MH. Mitogen-activated protein kinase pathways. Curr Opin Cell Biol. 1997;9:180–86.

Roy S, Bhattacharya S. Arsenic-induced histopathology and synthesis of stress proteins in liver and kidney of Channa punctatus. Ecotox Environ Saf. 2006;65:218–29.

Sambrook J, Fritsch EF, Maniatis T. Molecular cloning—a laboratory manual. 2nd ed. Cold Spring Harbor, New York: Cold Spring Harbor Laboratory; 1989.

Seok SH, Baek MW, Lee HY, Kim DJ, Na YR, Noh YR, et al. Arsenite-induced apoptosis is prevented by antioxidants in zebra fish liver cell line. Toxicol in Vitro. 2007;21:870–7.

Shimano K, Satake M, Okaya A, Kitanaka J, Kitanaka N, Takemura M, et al. Hepatic oval cell have the side population phenotype defined by expression of ATP binding cassette transporter ABCG2/BCRP1. American J Pathol. 2003;163(1):3–9.

Snedecor GW, Cochran WG. Statistical methods. 6th ed. Iowa: The Iowa State University Press; 1967.

Subjeck JR, Sciandra JJ, Johnson RJ. Heat shock proteins and thermotolerance; a comparison of induction kinetics. Br J Radiol. 1982;55:579–84.

Sun X-M, MacFarlane M, Zhuang J, Wolf BB, Green DR, Cohen GM. Distinct caspase cascade are initiated in receptor-mediated and chemical-induced apoptosis. J Biol Chem. 1999;274:5053–60.

Supino R. MTT assays. In: O'Hare S, Atterwill CK, editors. In vitro toxicity testing protocols. Totowa, New Jersey: Humana; 1995. p. 137–49.

Trosko JE. Human stem cells as targets for the aging and diseases of aging processes. Med Hypotheses. 2003;60:439–47.

Tsujimoto Y, Shimizu S. Bcl-2 family: life-or-death switch. FEBS Lett. 2001;466:6–10.

Wang X. The expanding role of mitochondria in apoptosis. Genes Dev. 2002;15:2922–33.

Wang K, Yin XM, Chao DT, Milliman CL, Korsmeyer SJ. BID: a novel BH3 domain-only death agonist. Genes Dev. 1996;10:2859–69.

Waskiewicz AJ, Cooper JA. Mitogen and stress response pathways: MAP kinase cascades and phosphatase regulation in mammals and yeast. Curr Opin Cell Biol. 1995;7:798–805.

Yin XM, Wang K, Gross A, Zhao Y, Zinkel S, Klocke B, et al. Bid-deficient mice are resistant to Fas-induced hepatocellular apoptosis. Nature 1999;400:886–91.